

# 硫化铅量子点辅助近红外二区荧光成像技术在活体应用中的研究进展

李慧<sup>1</sup>,朱丽君<sup>1</sup>,古丽妮尔·阿里木<sup>1</sup>,闫婷<sup>1</sup>,张学良<sup>2</sup>,努尔尼沙·阿力甫<sup>2</sup>

1.新疆医科大学公共卫生学院,新疆乌鲁木齐 830011; 2.新疆医科大学医学工程技术学院,新疆乌鲁木齐 830011

**【摘要】**近红外二区(NIR-II, 900~1 700 nm)的光相较于传统可见光(400~700 nm)和近红外一区(NIR-I, 700~900 nm)的光,波长更长,生物组织内传播时散射更小。因此,NIR-II 荧光成像技术在活体生物组织内具有深层穿透能力和高时空分辨率成像等优点。发射NIR-II 荧光的纳米探针备受研究者们的关注,其中硫化铅(PbS)量子点凭借尺寸可调、波段可调、易被修饰和量子产率高等优势成为生物医学活体成像的研究热点,如心脑血管和肿瘤等多种疾病的动物造影实验。本文介绍PbS 量子点的荧光特性和合成方法,概述NIR-II 窗口下 PbS 量子点基于多种物质的修饰,在胃肠道、血管、肿瘤、淋巴结等生物活体组织内荧光成像的应用,为探索该成像模式下未来发展潜力做铺垫。

**【关键词】**硫化铅量子点;近红外二区;荧光纳米探针;生物应用;综述

**【中图分类号】**R445;R318

**【文献标志码】**A

**【文章编号】**1005-202X(2023)01-0054-07

## Advances in *in vivo* application of lead sulfide quantum dots assisted NIR-II fluorescence imaging technology

LI Hui<sup>1</sup>, ZHU Lijun<sup>1</sup>, ALIMU Gulinigaer<sup>1</sup>, YAN Ting<sup>1</sup>, ZHANG Xueliang<sup>2</sup>, ALIFU Nuernisha<sup>2</sup>

1. School of Public Health, Xinjiang Medical University, Urumqi 830011, China; 2. School of Medical Engineering and Technology, Xinjiang Medical University, Urumqi 830011, China

**Abstract:** Compared with the light in the traditional visible region (400-700 nm) and in the near-infrared spectral region I (NIR-I, 700-900 nm), the light in the near-infrared spectral region II (NIR-II, 900-1 700 nm) has longer wavelength and smaller scattering during propagation within biological tissues. NIR-II fluorescence imaging technology shows the advantages of deep penetrating capability in *in vivo* biological tissues and high spatiotemporal resolution. With the development of nanotechnology, NIR-II fluorescence emissive nanoprobe are gradually developed. Lead sulfide (PbS) quantum dots have become the research hotspot because of their advantages of adjustable size, adjustable bands, easy to modify and extremely high quantum yield. In recent years, PbS nanoprobe assisted NIR-II fluorescence imaging technology exerted a huge impact on the biomedical field, especially the animal imaging experiments of cardio-cerebrovascular, tumors and other many diseases. Herein the fluorescence properties and synthesis methods of PbS quantum dots are introduced, and the *in vivo* applications of PbS quantum dots under the modifications of a variety of substances are summarized, and an overview of PbS quantum dots assisted NIR-II fluorescence imaging in *in vivo* biological tissues such as the gastrointestinal tract, blood vessels, tumors, lymph nodes is gave, which paves the way for exploring the future potential of this imaging model.

**Keywords:** lead sulfide quantum dot; near-infrared spectral region II; fluorescence nanoprobe; bio-medical application; review

## 前言

传统医学影像技术,如磁共振成像(MRI)、电子计算机断层扫描(CT)、多层计算机断层扫描(MDCT)和正电子发射计算机断层扫描(PET)等成像技术,凭借非侵入性的优势广泛应用于当前生物医学成像中<sup>[1]</sup>。MDCT是改善CT分辨率和成像效果的新技术,电离辐射的副作用仍未完全消除<sup>[2]</sup>。MRI

**【收稿日期】**2022-11-04

**【基金项目】**国家自然科学基金(82060326, 62035011);新疆维吾尔自治区自然科学基金(2020D01C151)

**【作者简介】**李慧,硕士研究生,主要研究方向:生物医学光子学,E-mail: 2583327307@qq.com

**【通信作者】**努尔尼沙·阿力甫,博士,副教授,博士生导师,主要研究方向:生物医学光子学,E-mail: 11530034@zju.edu.cn

在心血管的动力学、造影和成像分布等能力优于CT, 提供清晰度有限的2D平面图像未包含实时动态信息<sup>[3]</sup>。由此可见, 现阶段生物医学成像仍需操作简便、具有高灵敏和时空分辨率, 同时兼具对人体副作用小以及能特异性实时识别的新型成像技术。研究者们通过比较生物组织在可见光(400~700 nm)、近红外一区(NIR-I, 700~900 nm)和近红外二区(NIR-II, 900~1 700 nm)等3种不同波段下的成像潜力, 发现NIR-II波段由于高灵敏度和时空分辨率、无电离辐射、穿透能力强、极低的自荧光和光散射小等优势, 在增加图像信噪比、凸显病灶边缘和提示可靠的生理变化过程等具有显著的优势<sup>[4-6]</sup>。目前, NIR-II荧光成像技术应用于癌症造影、靶向载药、可控释药、抑制肿瘤生长和实时监测等生物医学研究中并取得了初步成效<sup>[7-9]</sup>。Hu等<sup>[10]</sup>成功实践了NIR-II荧光成像技术应用于人体肝肿瘤切除手术, 加快了近红外荧光成像全面应用临床医学的进程。但是NIR-II荧光穿透组织深度的突破仍被限制, 因此, 探讨发射明亮荧光的纳米探针以获取高分辨率生物造影至关重要。

用于生物医学领域中的荧光纳米探针主要分为有机纳米材料和无机纳米材料<sup>[8]</sup>。其中, 有机荧光团包括小分子染料<sup>[11]</sup>、小分子染料络合物<sup>[12]</sup>、有机纳米小分子染料<sup>[13]</sup>和纳米半导体聚合物颗粒<sup>[14]</sup>等; 无机纳米材料分为碳纳米管<sup>[15]</sup>、半导体量子点<sup>[16]</sup>、稀土纳米材料<sup>[17]</sup>、共轭聚合物<sup>[18]</sup>等。与有机纳米材料相比, 无机纳米材料硫化铅(PbS)量子点应用于光电探测器<sup>[19]</sup>、发光二极管<sup>[20]</sup>、太阳能电池<sup>[21]</sup>等领域的同时, 其优越的光物理特性也备受生物医学研究者的关注, 如PbS纳米探针更易功能化、发射出明亮的荧光、

宽场激发光、发射波长和直径可调、量子产率高等显著特点, 展现了量子点在荧光成像和临床诊疗的应用前景<sup>[22-23]</sup>。因此, 本综述总结了PbS量子点的光学特性和合成方法, 概述了国内外学者使用PbS量子点辅助NIR-II荧光在胃肠道、血管、肿瘤、淋巴结等生物成像技术的研究进展, 填补了该领域进展介绍的空白。

## 1 PbS量子点的光学特性和合成方法

### 1.1 光学特性

PbS量子点是IV-VI族、立方体结构且直径在20 nm以下的准零维纳米材料, 在生物医学成像和生物传感器等领域的研究潜力极大<sup>[24]</sup>。表1总结了NIR-II结合不同外部包裹的PbS量子点在血管、淋巴、肿瘤和胃肠道等生物组织的荧光性质。对比有机荧光染料, PbS量子点拥有以下特性:(1)带隙能量窄(0.41 eV), 并且激子波尔半径为18 nm, 具有宽场激发光谱和明亮的发射光谱, 能够提高时空分辨率; (2)生物兼容性和表面修饰性强, 表面包覆生物大分子、有机和无机材料后能够实时活体造影和靶向识别肿瘤; (3)荧光强度随着PbS量子点的物理尺寸和包覆物质而变化, 物理尺寸可以根据反应条件变化而变化, 如反应温度、pH、反应物的选择和浓度; (4)斯托克斯位移大(发射波长和激发波长的差值), 范围为300~400 nm, 可以在低荧光波段激发光下, 连续、多次荧光造影; (5)在生物组织内, 光子的吸收、散射低, 荧光渗透和抗光漂白能力强; (6)量子产率高, 体内、外的荧光稳定性强; (7)能够结合有机染料、多波段光谱和常规电离辐射成像设备完成生物组织的造影和诊疗等研究。

表1 PbS量子点辅助NIR-II荧光成像的生物应用

Table 1 PbS quantum dots-assisted NIR-II fluorescence imaging in biological application

量子点	发射荧光/nm	直径/nm	量子产率/%	生物应用	参考文献
PbS@CdS@OPA	1 650	18.2	2.2-22 <sup>a</sup>	血管、肿瘤(MC38)	文献[25]
PbS@CdS@SiO <sub>2</sub> @F-127	1 155	68	5.79 <sup>a,d</sup>	血管、胃肠道	文献[26]
PbS@Ag <sub>2</sub> Se@V&C	1 600	150	-	血管	文献[27]
PbS@CdS@PEG	1 600	6.8	2-20 <sup>a</sup>	血管	文献[28]
PbS@CdS/PbS@CdS@FA	1 080/1 280	15.0/16.9	16.8 <sup>a,c</sup> /4.1 <sup>a</sup>	肿瘤(HeLa)	文献[29]

量子产率的计算根据如下所示:<sup>a</sup>近红外染料IR-26=0.05-0.5%;<sup>b</sup>近红外染料IR125在乙醇溶液中;量子产率的测量是在<sup>c</sup>PBS缓冲液和<sup>d</sup>水中

### 1.2 合成方法

在生物医学研究中, 热注射法作为国内外学者合成PbS量子点的主要方法<sup>[28,31,34]</sup>, 可以合成单分散、

粒径窄和量子产率高的量子点。在合成之前, 需要在油胺、油酸或者三辛基膦等有机配体的环境下制备铅前体和硫前体两种溶液(表2)。有机配体也是

表面活性剂,能够有效覆盖在量子点表面以维持胶体稳定性并分布均匀。其中,油酸和三辛基膦或者油酸作为热注射法的配体时,能够保持量子点的初始结构和荧光稳定性;油胺配体在反应中引发的Ostwald熟化,导致量子点物理直径两极化分布,降低分散性;油酸和三辛基膦配体封装的PbS量子点的荧光强度是油胺或油酸封装的两倍<sup>[35]</sup>。热注射法在创

建保护气和高温环境后,将硫前驱体注入到铅前驱体中,剧烈搅拌混合的两种溶液,同时监测合成PbS量子点的发射峰。而调节反应温度、pH、前体溶液成分和浓度等条件均可改变量子点的直径、发射光谱和量子产率。冷水降温或加入乙醇、正乙烷等猝灭剂终止反应后,应用离心法沉淀、油酸去除过量的硫前体等步骤以获取高分散性PbS量子点。

表2 PbS量子点的合成材料和反应环境

Table 2 Synthetic materials and reaction settings of PbS quantum dots

铅前体溶液	硫前体溶液	反应条件	沉淀剂	悬浮剂	参考文献
氯化铅、油胺	硫磺、油胺	氩气、160 °C	-	ODE	文献[25]
氯化铅、油胺	硫磺、油胺	110 °C	乙醇	氯仿	文献[27]
氯化铅、油胺	硫磺、油胺	氮气、100 °C	乙醇	己烷	文献[28]
氧化铅、TOP、油酸	HAH	真空、110 °C	乙醇	-	文献[30]
醋酸铅、油酸	(TMS) <sub>2</sub> S、TOP	氮气、100 °C	甲醇	甲苯	文献[31]
氯化铅、油胺	硫磺、油胺	氮气、100 °C	乙醇、甲苯	甲苯	文献[31]
氯化铅、油胺	硫磺、油胺	氩气、160 °C	-	ODE	文献[32]
氯化铅、油胺	硫磺、油胺	氩气、160 °C	乙醇	甲苯、ODE	文献[33]
氯化铅、油胺、油酸	TBP、HAH	氩气、100~150 °C	甲醇	油胺、甲苯	文献[35]
醋酸铅、PAA	硫脲、二甘醇	210 °C	乙醇	(固体)	文献[36]
氯化铅、油胺、油酸	HAH、TBP	氩气、100 °C	甲醇	-	文献[37]
醋酸铅	硫化钠	pH=7.5、100 °C	-	-	文献[38]

HAH:六甲基二硅硫烷;TBP:三丁基膦;ODE:1-十八烯;PAA:聚丙烯酸;(TMS)<sub>2</sub>S:双(三甲基甲硅烷基)硫化物;TOP:三辛基膦

## 2 PbS纳米探针辅助NIR-II荧光造影技术在生物医学的应用

### 2.1 胃肠道造影

胃肠道疾病作为常见外科急性疾病,X射线、CT、超声检查(US)和MRI等影像技术是临床检查的常规手段,但仍然有严重的限制,如US非智能手持设备,对医疗技师熟练度的依赖和有限的灵敏度<sup>[39]</sup>。

PbS量子点辅助NIR-II荧光成像技术具有弥补以上短板的潜力。Liu等<sup>[36]</sup>已经使用PbS造影剂完成X射线和CT造影活体胃肠道的试验,证实PbS量子点对比临床常用钡餐更具有纳米造影剂的潜力。

为更全面验证PbS造影剂的应用能力,Zebibula等<sup>[26]</sup>合成了二氧化硅包裹和双亲性聚合物F-127修饰PbS@CdS@SiO<sub>2</sub>@F-127量子点(简称NPs),这种包覆方式不仅提高了量子点的生物兼容性和水溶性,而且实现了脑血管、胃肠道和全身等造影实验。在体外胃肠道成像实验中,NPs在pH=1的体外强酸

环境下,24 h后仍然保留65%的荧光强度,证明该量子点具有荧光稳定性优势;为探讨NPs的体内生物兼容性、显影效果和排泄途径,该课题组采用尾静脉注射量子点水溶液的方式,观察785 nm激发光下的活体全身成像图,发现NPs的荧光可以渗透3~5 mm的胃肠道组织,并且NPs在4.5 h后从粪便安全排出(图1a)。该量子点生物兼容性强、操作简单、时空分辨率高和超小纳米尺寸等优势为胃肠道成像造影剂辅助光学技术铺平道路,拓宽了生物医学应用领域。

### 2.2 血管造影

血管不仅是脏器的供血通路,维持生命体征,而且能控制周围器官的生长<sup>[40]</sup>。脑静脉血栓作为发病率极高的心脑血管疾病<sup>[41]</sup>,需要在高精度靶向造影辅助下,确定血栓分布和数量<sup>[42]</sup>。因此,Yang等<sup>[27]</sup>合成了V&C/PbS@Ag<sub>2</sub>Se量子点(图1b),其中,过氧亚硝酸盐(ONOO<sup>-</sup>)作为早期缺血性卒中标志物,可以氧化近红外花青素荧光染料(Cy 7.5)的同时,破除Cy 7.5和PbS@Ag<sub>2</sub>Se量子点竞争吸收激发光的关系,

结合VCAM1结合钛作为靶点,引导V&C/PbS@Ag<sub>2</sub>Se量子点在血栓处的双重发光,达到快速识别病灶并产生1600 nm发射峰的显影效果,呈现了特异性和高

灵敏度的血栓造影,为诊断早期缺血性脑卒中奠定基础。

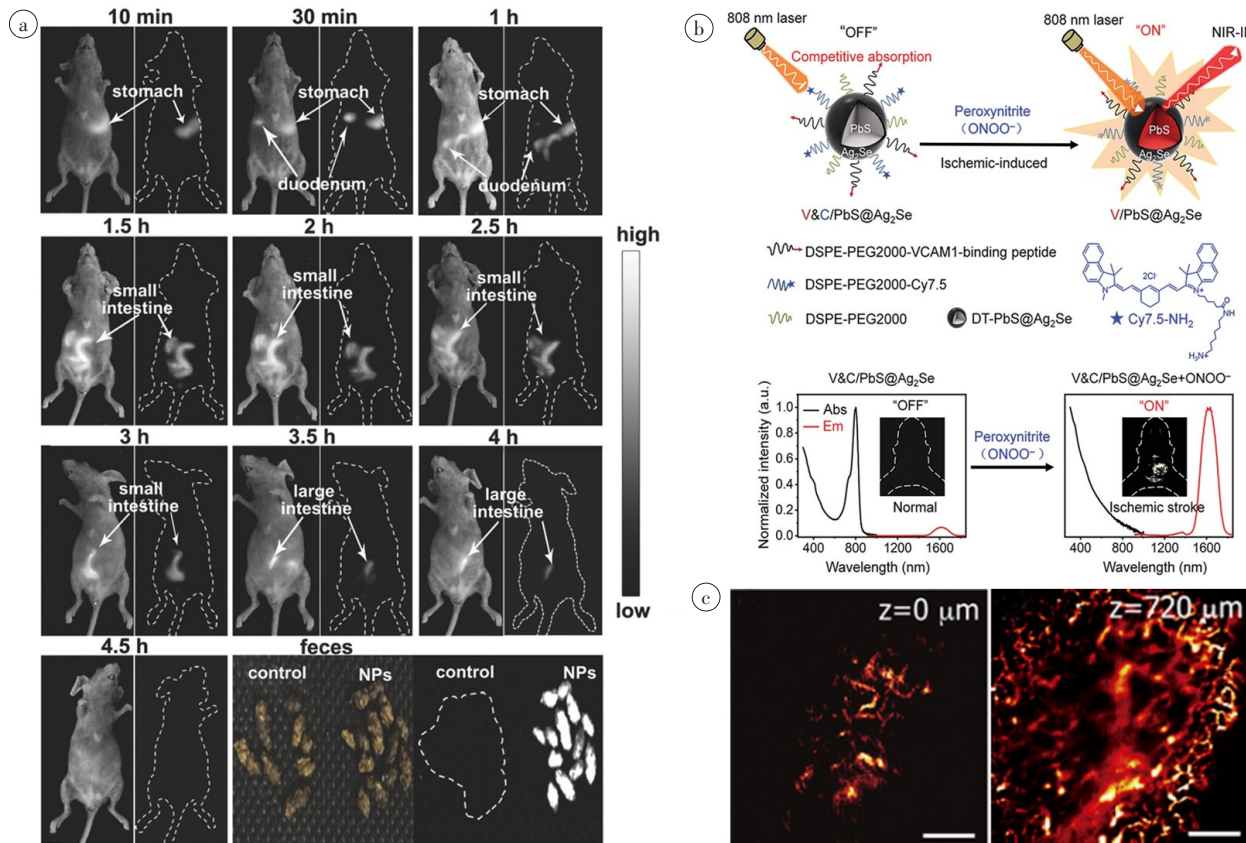


图1 PbS量子点在胃肠道和血管造影中的应用

Figure 1 PbS quantum dots for gastrointestinal and angiographic applications

a:静脉注射NPs水溶液后的胃肠道荧光图<sup>[26]</sup>;b:V&C/PbS@Ag<sub>2</sub>Se量子点的“开-关”体系<sup>[27]</sup>;c:PbS@CdS量子点的结肠癌血管造影图<sup>[25]</sup>

外周动脉疾病由于血流动力学障碍而导致跛行或者截肢<sup>[43-44]</sup>。Ma等<sup>[28]</sup>为获取血管动力的高时空分辨率图像,开发CdS量子点和双亲性聚合物包裹PbS量子点(简称PbS@CdS@PEG)的显影材料,双层包裹提升了PbS量子点的水相性和生物兼容性,而且发射出1600 nm的明亮荧光。对比常用血管造影剂单壁碳纳米管在NIR-IIa(1300~1400 nm)的显影效果,NIR-IIb(1500~1700 nm)下PbS@CdS@PEG量子点的造影图不仅呈现极低的生物自荧光和光散射,而且能够实时监测血液动力学和跟踪新生血管的光学特性。

Zhang等<sup>[25]</sup>合成了聚乙二醇修饰的PbS@CdS量子点,不仅拥有800 nm的斯托克斯位移和1650 nm的发射荧光,而且7 h的药物半衰期可以较快地消除体内量子点,进一步降低毒性效应。透过共聚焦显微镜可以看到荧光穿透并呈现了肿瘤表面与内部的血管结构,其活体透皮实时造影深度为720 μm,

最深可达1.2 mm(图1c),实现了活体小鼠无创、高分辨率的透皮血流监控,表明PbS量子点具有实现“透明病理”和精准医疗的优势。对比胃肠道成像策略,两项工作呈现的荧光穿透组织深度和药物消除时间仍有进一步改善的空间<sup>[36]</sup>。

### 2.3 肿瘤造影

癌症的精准诊疗是医学攻坚的关键难题<sup>[45]</sup>。目前临幊上使用MRI和CT等电离辐射成像以及生化生物标志物可辅助肿瘤诊断<sup>[46]</sup>,但靶向造影肿瘤的潜力未被开发。Jeong等<sup>[29]</sup>利用叶酸受体在肿瘤细胞表面过表达<sup>[47-48]</sup>和PbS量子点的简单表面修饰性<sup>[49]</sup>完成了精准造影肿瘤。将叶酸偶联到PbS@CdS量子点(简称FA-QDs)表面,对比未偶联叶酸的PbS@CdS量子点,FA-QDs能够识别叶酸受体阳性的子宫颈癌细胞,并且荧光稳定性长超过一周以上,证明了PbS量子点能够表面修饰功能分子并特异性靶向识别肿瘤。

人表皮生长因子受体2(HER2)<sup>[50-51]</sup>和三明治式电化学免疫传感器<sup>[52]</sup>分别可以实现靶向识别肿瘤和定量诊断肿瘤。Lah等<sup>[53]</sup>将三明治免疫传感器和偶联HER2抗体的PbS量子点结合,用于人血清中HER2的检测,为乳腺癌诊断提供一种新的思路。除了便捷靶向定位乳腺肿瘤外,Depalo等<sup>[30]</sup>展示了二氧化硅包覆、环精氨酸-甘氨酸-天冬氨酸肽修饰后的PbS量子点,可以特异性识别皮肤肿瘤过表达的整合素 $\alpha V\beta 3$ ,成功实现人黑素瘤细胞的靶向识别。

基质金属蛋白酶(MMP)是机体调节细胞增殖和伤口愈合的蛋白酶<sup>[54]</sup>,但MMP的过表达可作为诊断肿瘤<sup>[50]</sup>和血管性认知障碍<sup>[55-56]</sup>等疾病的标志物。与正常组织成像相比,Jeong等<sup>[57]</sup>制作的多层MMP封装的PbS纳米探针在结直肠癌荷瘤小鼠肿瘤部位的荧光强度,10 min内增长了3倍,实现了高信噪比、非侵入和高分辨率的肿瘤微环境造影。

PbS纳米探针的发光成像和靶向定位特性在众多生物材料的修饰下大大提升,除了使用不同配体修饰PbS纳米探针,Yang等<sup>[31]</sup>将超顺磁性氧化铁纳米粒子(SPIO)和PbS@CdS量子点组装成超级纳米粒子,荧光不仅能渗透14 mm的生物组织,而且热效应提升了7倍,为光、热双模态热效应诊疗乳腺癌提供了实验数据支撑。

#### 2.4 淋巴结造影

为判断乳腺癌、子宫内膜癌等多种癌症是否扩散并完成肿瘤分期,淋巴结造影是主要的判定依

据<sup>[58-59]</sup>,MRI和PET/CT通过淋巴结成像完成肿瘤分期和诊断的准确度均低于87%<sup>[60]</sup>。为实现高灵敏度的淋巴结成像,Tian等<sup>[32]</sup>开发了双光谱成像体系,可应用于转移和非转移肿瘤的造影和手术引导。该工作采用近红外染料ICG和合成的PbS@CdS量子点结合的设计,分别在NIR-IIa和NIR-IIb窗口实现乳腺癌定位和肿瘤浸润的前哨淋巴结成像,并且PbS@CdS量子点与美国食品药品监督管理局(FDA)批准临床使用的吲哚菁绿(ICG)相比,荧光强度能提升20倍。双NIR-II光谱成像体系在连续激光照射5 h的情况下,几乎不出现组织漂白和光散射,更加说明PbS量子点具有功能性结合和实现高时空分辨率淋巴结可视化的极大潜力,为肿瘤分期提供有力的凭证。

同样与FDA批准临床使用ICG造影效果相比,Ma等<sup>[33]</sup>合成了多种双亲性聚合物[1-十八烯马来酸酐、多臂PEG衍生物、聚(丙烯酸)和聚乙二醇单甲醚]修饰的PbS@CdS量子点(简称P3-QDs)。如图2a所示,P3-QDs在NIR-II窗口中,不仅发射峰为1 600 nm,而且图像的信噪比达到170,其成像效果远超临床使用的ICG荧光染料。该课题组在此设计的基础上,将相同包裹方法的SPIO(简称P3-SPIO)用于全身近红外成像(图2b),确认了纳米粒子主要聚集地(肝脏和脾脏)以及该种修饰方法是提升水相溶解性和生物兼容性的通用理念。

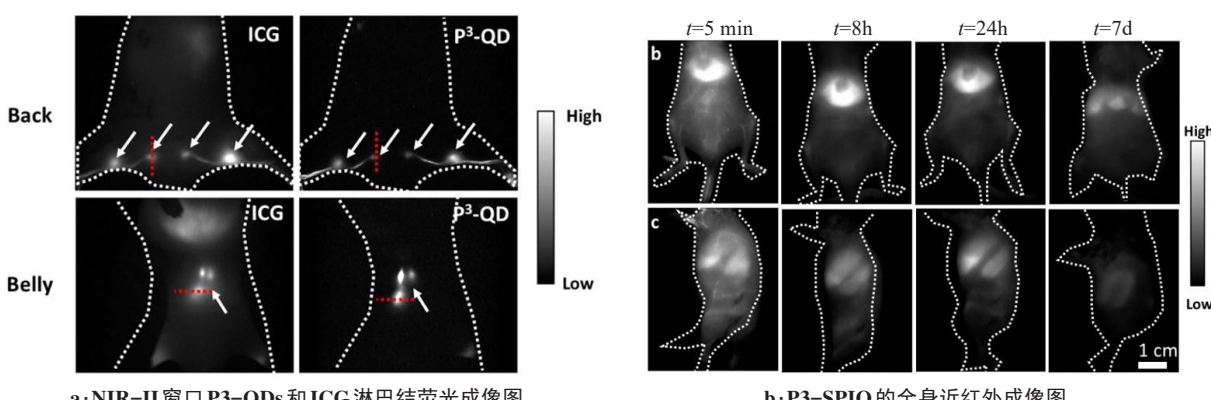


图2 ICG和P3-QDs的淋巴结造影图,以及P3-SPIO的全身近红外成像图<sup>[33]</sup>

Figure 2 Lymph node imaging with ICG and P3-QDs, and near-infrared imaging of P3-SPIO in the whole body<sup>[33]</sup>

### 3 总结与展望

本文概述了NIR-II生物窗口下PbS纳米探针的多种包覆方式的设计和活体内荧光成像应用。在不同设计方法和生物组织中,PbS纳米探针表现出不同的发射光谱、靶向识别和成像能力。随着NIR-II成像

和纳米材料在医学领域癌症造影、癌症药物运载体、肿瘤治疗等方面的发展,荧光引导手术不仅能够简化操作,而且可实时造影。由此可见,NIR-II光学辅助下的术前造影诊断和术中指引肿瘤分布拥有巨大的潜力。与ICG辅助NIR-I的成像相比,PbS量子

点辅助NIR-II成像凭借其无创、光散射低、高生物兼容性和时空分辨率、易表面修饰性等特点,在心脑血管、癌症、胃肠道和淋巴结等深层次生物组织成像中,充分发挥其优势。该项造影技术结合多种光谱成像方法,将为肿瘤发展和转移提供精准诊疗的理论依据,并且在手术中精准导向、完善预后,是未来基础和临床研究上拥有巨大潜力的纳米造影材料之一。

NIR-II生物窗口下PbS纳米探针造影技术仍有广阔的应用前景,例如进一步提高PbS纳米探针的光子转移灵敏度,可能会提供以亚毫秒时间分辨率和亚细胞空间分辨率双监测的技术支持,实现深层组织神经细胞群的神经活动造影的可能性,为研究神经系统疾病提供新思路。无创荧光成像在胚胎与器官的发育过程以及干细胞的追踪等基础生物学机制的研究也具有巨大的潜力,但从临床应用的角度考虑,仍要全面评估PbS纳米探针的特定代谢途径、长期生物毒性和体内兼容性。最后,为减少成像视场、分辨率和穿透深度等限制,大力开发和优化NIR-II成像设备性能也十分重要。

## 【参考文献】

- [1] Choi SH, Kim SY, Park SH, et al. Diagnostic performance of CT, gadoxetate disodium-enhanced MRI, and PET/CT for the diagnosis of colorectal liver metastasis: systematic review and meta-analysis[J]. *J Magn Reson Imaging*, 2018, 47(5): 1237-1250.
- [2] Agliati G, Schicchi N, Agostini A, et al. Radiation exposure related to cardiovascular CT examination: comparison between conventional 64-MDCT and third-generation dual-source MDCT [J]. *Radiol Med*, 2019, 124(8): 753-761.
- [3] Liu DT, Fan ZM, Li Y, et al. Quantitative study of abdominal blood flow patterns in patients with aortic dissection by 4-dimensional flow MRI [J]. *Sci Rep*, 2018, 8(1): 1-8.
- [4] Yu XM, Feng Z, Cai ZC, et al. Deciphering of cerebrovasculatures via ICG-assisted NIR-II fluorescence microscopy [J]. *J Mater Chem B*, 2019, 7(42): 6623-6629.
- [5] Cao J, Zhu BL, Zheng KF, et al. Recent progress in NIR-II contrast agent for biological imaging [J]. *Front Bioeng Biotechnol*, 2020: 487. DOI: 10.3389/fbioe.2019.00487.
- [6] Li DL, Liu Q, Qi QR, et al. Gold nanoclusters for NIR-II fluorescence imaging of bones [J]. *Small*, 2020, 16(43): 2003851.
- [7] Zhao P, Xu Q, Tao J, et al. Near infrared quantum dots in biomedical applications: current status and future perspective [J]. *Wires Nanomed Nanobi*, 2018, 10(3): 1483.
- [8] He SQ, Song J, Qu JL, et al. Crucial breakthrough of second near-infrared biological window fluorophores: design and synthesis toward multimodal imaging and theranostics [J]. *Chem Soc Rev*, 2018, 47(12): 4258-4278.
- [9] Ding DD, Li S, Xu H, et al. X-ray-activated simultaneous near-infrared and short-wave infrared persistent luminescence imaging for long-term tracking of drug delivery [J]. *ACS Appl Mater Interfaces*, 2021, 13(14): 16166-16172.
- [10] Hu ZH, Fang C, Li B, et al. First-in-human liver-tumour surgery guided by multispectral fluorescence imaging in the visible and near-infrared-I/II windows [J]. *Nat Biomed Eng*, 2020, 4(3): 259-271.
- [11] Ding F, Li CL, Xu YL, et al. PEGylation regulates self-assembled small-molecule dye-based probes from single molecule to nanoparticle size for multifunctional NIR-II bioimaging [J]. *Adv Healthc Mater*, 2018, 7(23): e1800973.
- [12] Legault S, Fraser-Halberg DP, McAnelly RL, et al. Generation of bright monomeric red fluorescent proteins via computational design of enhanced chromophore packing [J]. *Chem Sci*, 2022, 13(5): 1408-1418.
- [13] Cai Y, Si WL, Huang W, et al. Organic dye based nanoparticles for cancer phototheranostics [J]. *Small*, 2018, 14(25): e1704247.
- [14] Cao ZY, Feng LZ, Zhang GB, et al. Semiconducting polymer-based nanoparticles with strong absorbance in NIR-II window for *in vivo* photothermal therapy and photoacoustic imaging [J]. *Biomaterials*, 2018, 155: 103-111.
- [15] Omparetti EJ, Pedrosa VA, Kaneno R. Carbon nanotube as a tool for fighting cancer [J]. *Bioconjug Chem*, 2017, 29(3): 709-718.
- [16] Vyshnava SS, Pandluru G, Kumar KD, et al. Biocompatible Ni-doped CdSe/ZnS semiconductor nanocrystals for cellular imaging and sorting [J]. *Luminescence*, 2022, 37(3): 490-499.
- [17] Zhao YZ, Hao XT, Lu W, et al. Facile preparation of double rare earth-doped carbon dots for MRI/CT/FI multimodal imaging [J]. *Acs Appl Nano Mater*, 2018, 1(6): 2544-2551.
- [18] Meng ZH, Hou WY, Zhou H, et al. Therapeutic considerations and conjugated polymer-based photosensitizers for photodynamic therapy [J]. *Macromol Rapid Commun*, 2018, 39(5): 1700614.
- [19] Yin X, Zhang C, Guo Y, et al. PbS QD-based photodetectors: future-oriented near-infrared detection technology [J]. *J Mater Chem C Mater*, 2021, 9(2): 417-438.
- [20] Jung BK, Kim W, Oh SJ. Stable colloidal quantum dot-based infrared photodiode: multiple passivation strategy [J]. *J Korean Ceram Soc*, 2021, 58(5): 521-529.
- [21] Blachowicz T, Ehrmann A. Recent developments of solar cells from PbS colloidal quantum dots [J]. *Appl Sci*, 2020, 10(5): 1743.
- [22] Jin T, Imamura Y. Applications of highly bright PbS quantum dots to non-invasive near-infrared fluorescence imaging in the second optical window [J]. *Ecs J Solid State Sc*, 2015, 5(1): R3138.
- [23] Bera A, Mandal D, Goswami PN, et al. Generic and scalable method for the preparation of monodispersed metal sulfide nanocrystals with tunable optical properties [J]. *Langmuir*, 2018, 34(20): 5788-5797.
- [24] Zhou BZ, Liu MJ, Wen YW, et al. Atomic layer deposition for quantum dots based devices [J]. *Opto-electron Adv*, 2020, 3(9): 14.
- [25] Zhang MX, Yue JY, Cui R, et al. Bright quantum dots emitting at approximately 1600 nm in the NIR-IIb window for deep tissue fluorescence imaging [J]. *Proc Natl Acad Sci U S A*, 2018, 115(26): 6590-6595.
- [26] Zebibula A, Alifu N, Xia LQ, et al. Ultrastable and biocompatible NIR-II quantum dots for functional bioimaging [J]. *Adv Funct Mater*, 2018, 28(9): 1703451.
- [27] Yang XH, Wang Z, Huang HY, et al. A targeted activatable NIR-IIb nanoprobe for highly sensitive detection of ischemic stroke in a photothrombotic stroke model [J]. *Adv Healthc Mater*, 2021, 10(5): 2001544.
- [28] Ma ZR, Zhang MX, Yue JY, et al. Near-infrared IIb fluorescence imaging of vascular regeneration with dynamic tissue perfusion measurement and high spatial resolution [J]. *Adv Funct Mater*, 2018, 28(36): 1803417.
- [29] Jeong SW, Jung YB, Bok S, et al. Multiplexed *in vivo* imaging using size-controlled quantum dots in the second near-infrared window [J]. *Adv Healthc Mater*, 2018, 7(24): 1800695.
- [30] Depalo N, Corricelli M, De Paola I, et al. NIR emitting nanoprobes based on cyclic RGD motif conjugated PbS quantum dots for integrin-targeted optical bioimaging [J]. *ACS Appl Mater Interfaces*, 2017, 9(49): 43113-43126.
- [31] Yang F, Skripka A, Tabatabaei MS, et al. Multifunctional self-assembled supernanoparticles for deep-tissue bimodal imaging and amplified dual-mode heating treatment [J]. *ACS Nano*, 2019, 13(1): 408-420.
- [32] Tian R, Ma HL, Zhu SJ, et al. Multiplexed NIR-II probes for lymph node-invaded cancer detection and imaging-guided surgery [J]. *Adv Mater*, 2020, 32(11): 1907365.
- [33] Ma ZR, Wang FF, Zhong YT, et al. Advancing nanomedicine with cross-link functionalized nanoparticles for rapid excretion [J]. *Angew Chem Int Ed Engl*, 2020, 59(46): 20552-20560.
- [34] Tsukasaki Y, Komatsuzaki A, Mori Y, et al. A short-wavelength infrared emitting multimodal probe for non-invasive visualization of phagocyte

- cell migration in living mice[J]. *Chem Commun (Camb)*, 2014, 50(92): 14356-14359.
- [35] Zhao HG, Wang DF, Chaker M, et al. Effect of different types of surface ligands on the structure and optical property of water-soluble PbS quantum dots encapsulated by amphiphilic polymers[J]. *J Phys Chem C*, 2011, 115(5): 1620-1626.
- [36] Liu Z, Ran X, Liu JH, et al. Non-toxic lead sulfide nanodots as efficient contrast agents for visualizing gastrointestinal tract[J]. *Biomaterials*, 2016, 100: 17-26.
- [37] Imamura Y, Yamada S, Tsuboi S, et al. Near-infrared emitting PbS quantum dots for *in vivo* fluorescence imaging of the thrombotic state in septic mouse brain[J]. *Molecules*, 2016, 21(8):1080.
- [38] Chen J, Kong YF, Wang W, et al. Direct water-phase synthesis of lead sulfide quantum dots encapsulated by beta-lactoglobulin for *in vivo* second near infrared window imaging with reduced toxicity[J]. *Chem Commun (Camb)*, 2016, 52(21): 4025-4028.
- [39] Van Zelst JC, Mann RM. Automated three-dimensional breast US for screening: technique, artifacts, and lesion characterization [J]. *Radiographics*, 2018, 38(3): 663-683.
- [40] Majesky MW. Vascular development[J]. *Arterioscler Thromb Vasc Biol*, 2018, 38(3): e17-e24.
- [41] Capecchi M, Abbattista M, Martinelli I. Cerebral venous sinus thrombosis[J]. *J Thromb Haemost*, 2018, 16(10): 1918-1931.
- [42] Diener HC, Hankey GJ. Primary and secondary prevention of ischemic stroke and cerebral hemorrhage: JACC focus seminar[J]. *J Am Coll Cardiol*, 2020, 75(15): 1804-1818.
- [43] Signorelli SS, Scuto S, Marino E, et al. Oxidative stress in peripheral arterial disease(PAD) mechanism and biomarkers[J]. *Antioxidants*, 2019, 8(9): 367.
- [44] Gottsäter A. Antithrombotic treatment in lower extremity peripheral arterial disease[J]. *Front Cardiovasc Med*, 2021, 8: 773214.
- [45] Fidler MM, Bray F, Soerjomataram I. The global cancer burden and human development: a review[J]. *Scand J Public Health*, 2018, 46(1): 27-36.
- [46] Jafari SH, Saadatpour Z, Salmanejad A, et al. Breast cancer diagnosis: imaging techniques and biochemical markers[J]. *J Cell Physiol*, 2018, 233(7): 5200-5213.
- [47] Nawaz FZ, Kipreos ET. Emerging roles for folate receptor FOLR1 in signaling and cancer[J]. *Trends Endocrinol Met*, 2022, 33(3): 159-174.
- [48] Samadian H, Merzel RL, Dyson JM, et al. Anti-tumor effect of folate-binding protein: *in vitro* and *in vivo* studies[J]. *Mol Pharm*, 2022, 19(3): 843-852.
- [49] Kennehan ER, Munson KT, Doucette GS, et al. Dynamic ligand surface chemistry of excited PbS quantum dots[J]. *J Phys Chem Lett*, 2020, 11(6): 2291-2297.
- [50] Oh DY, Bang YJ. HER2-targeted therapies-a role beyond breast cancer [J]. *Nat Rev Clin Oncol*, 2020, 17(1): 33-48.
- [51] Kunte S, Abraham J, Montero AJ. Novel HER2-targeted therapies for HER2-positive metastatic breast cancer[J]. *Cancer*, 2020, 126(19): 4278-4288.
- [52] Fan DW, Ren X, Wang HY, et al. Ultrasensitive sandwich-type photoelectrochemical immunosensor based on CdSe sensitized La-TiO<sub>2</sub> matrix and signal amplification of polystyrene@Ab2 composites [J]. *Biosens Bioelectron*, 2017, 87: 593-599.
- [53] Lah ZM, Ahmad SA, Zaini MS, et al. An electrochemical sandwich immunoassay for the detection of HER2 using antibody-conjugated PbS quantum dot as a label[J]. *J Pharm Biomed Anal*, 2019, 174: 608-617.
- [54] Pandit A, Begum Y, Saha P, et al. Approaches towards targeting matrix metalloproteases for prognosis and therapies in gynecological cancer: microRNAs as a molecular driver[J]. *Front Oncol*, 2021, 11: 720622.
- [55] Huang H. Matrix metalloproteinase-9(MMP-9) as a cancer biomarker and MMP-9 biosensors: recent advances[J]. *Sensors*, 2018, 18(10): 3249.
- [56] Mondal S, Adhikari N, Banerjee S, et al. Matrix metalloproteinase-9 (MMP-9) and its inhibitors in cancer: a minireview[J]. *Eur J Med Chem*, 2020, 194: 112260.
- [57] Jeong S, Song J, Lee W, et al. Cancer-microenvironment-sensitive activatable quantum dot probe in the second near-infrared window[J]. *Nano Lett*, 2017, 17(3): 1378-1386.
- [58] Veronesi P, Corso G. Standard and controversies in sentinel node in breast cancer patients[J]. *Breast*, 2019, 48: S53-S56.
- [59] Varol C, Sagi I. Phagocyte-extracellular matrix crosstalk empowers tumor development and dissemination[J]. *FEBS J*, 2018, 285(4): 734-751.
- [60] Sarabhai T, Schaarschmidt BM, Wetter A, et al. Comparison of <sup>18</sup>F-FDG PET/MRI and MRI for pre-therapeutic tumor staging of patients with primary cancer of the uterine cervix[J]. *Eur J Nucl Med Mol Imaging*, 2018, 45(1): 67-76.

(编辑:陈丽霞)